

## Development of a particle injection system for impurity transport study in KSTARa)

H. Y. Lee, Suk-Ho Hong, JooHwan Hong, Seung Hun Lee, Siwon Jang, Juhyeok Jang, Taemin Jeon, Jae Sun Park, and Wonho Choe

Citation: [Review of Scientific Instruments](#) **85**, 11D862 (2014); doi: 10.1063/1.4886958

View online: <http://dx.doi.org/10.1063/1.4886958>

View Table of Contents: <http://scitation.aip.org/content/aip/journal/rsi/85/11?ver=pdfcov>

Published by the [AIP Publishing](#)

---

### Articles you may be interested in

[Rotation characteristics during the resonant magnetic perturbation induced edge localized mode suppression on the KSTARa\)](#)

Rev. Sci. Instrum. **85**, 11E413 (2014); 10.1063/1.4890402

[Design and fabrication of a multi-purpose soft x-ray array diagnostic system for KSTARa\)](#)

Rev. Sci. Instrum. **83**, 10E512 (2012); 10.1063/1.4734035

[Measurement of plasma current dependent changes in impurity transport and comparison with nonlinear gyrokinetic simulationa\)](#)

Phys. Plasmas **19**, 056110 (2012); 10.1063/1.3694113

[Active spectroscopic measurements using the ITER diagnostic systema\)](#)

Rev. Sci. Instrum. **81**, 10D725 (2010); 10.1063/1.3491293

[Measurement of poloidal velocity on the National Spherical Torus Experiment \(invited\)a\)](#)

Rev. Sci. Instrum. **81**, 10D724 (2010); 10.1063/1.3485027

---

**Nor-Cal Products**



Manufacturers of High Vacuum  
Components Since 1962

- Chambers
- Motion Transfer
- Flanges & Fittings
- Viewports
- Foreline Traps
- Feedthroughs
- Valves



[www.n-c.com](http://www.n-c.com)  
800-824-4166

## Development of a particle injection system for impurity transport study in KSTAR<sup>a)</sup>

H. Y. Lee,<sup>1</sup> Suk-Ho Hong,<sup>2</sup> Joohwan Hong,<sup>1</sup> Seung Hun Lee,<sup>1</sup> Siwon Jang,<sup>1</sup> Juhyeok Jang,<sup>1</sup> Taemin Jeon,<sup>1</sup> Jae Sun Park,<sup>1</sup> and Wonho Choe<sup>1, b)</sup>

<sup>1</sup>*Department of Physics, Korea Advanced Institute of Science and Technology, Daejeon 305-701, Republic of Korea and Fusion Plasma Transport Research Center, Daejeon 305-701, Republic of Korea*  
<sup>2</sup>*National Fusion Research Institute, Daejeon 305-806, Republic of Korea*

(Presented 2 June 2014; received 30 May 2014; accepted 23 June 2014; published online 25 September 2014)

A solid particle injection system is developed for KSTAR. The system has a compact size, compatibility with a strong magnetic field and high vacuum environment, and the capability to inject a small amount of solid particles with a narrow injection angle. The target flight-distance of 10 cm has been achieved with a particle loss rate of less than 10%. Solid impurity particles such as tungsten and carbon will be injected by this system at the midplane in KSTAR. The impurity transport feature will be studied with a soft X-ray array, a vacuum ultra-violet diagnostic, and Stand Alone Non-Corona code.  
 © 2014 AIP Publishing LLC. [<http://dx.doi.org/10.1063/1.4886958>]

### I. INTRODUCTION

High purity plasma is one of the principal requirements for achieving high fusion reaction rate in fusion plasmas. Since small effective charge ( $Z_{\text{eff}}$ ) is desirable for an efficient fusion yield.<sup>1,2</sup> In the International Thermonuclear Experimental Reactor (ITER), a full tungsten (W) divertor is going to be employed and impurity seeding, i.e., argon (Ar) or neon, which builds a radiative mantle, is proposed for the reduction of heat load on the divertor.<sup>3</sup> Therefore the effect of  $Z_{\text{eff}}$  on impurity transport is an important topic to be studied for ITER and future fusion devices.

In KSTAR, Ar impurity transport study has been performed.<sup>4</sup> Since KSTAR has succeeded extending H-mode pulse length to 15 s,<sup>5</sup> that allows us to study the impurity transport for long pulse H-mode plasmas in KSTAR with parameters for ITER relevant experiments. For impurity transport studies in KSTAR, a Soft X-ray (SXR) array<sup>6</sup> and an ITER proto-type Vacuum Ultra-Violet (VUV) diagnostic<sup>7</sup> have been utilized. Usually, a gas puffing system has been used for the trace impurity injection. It is difficult to achieve an accurate influx of Ar into the plasma with the gas puffing system. Instead of the gas puffing system, a pellet injection system,<sup>8</sup> an impurity powder dropper,<sup>9</sup> and a gun type impurity solid particle injector can be considered as the trace particle injection system. Among them, a gun type solid particle injection system can easily inject solid impurity particles without additional complicated safety issues, thus we have developed the particle injection system for KSTAR. In this study, we report the details on the design, the fabrication, and the test result of the particle injection system.

The particle injection system will be mounted on the manipulator, which is installed to a position 35 cm lower than

the midplane of the D-port. The manipulator radially moves to a location inside the vacuum vessel up to 10 cm away from the Last Closed Flux Surface (LCFS) for typical KSTAR discharges with major and minor radii being 1.8 m and 0.5 m, respectively. Therefore, a particle flight-distance is required longer than 10 cm from the particle injection system. Other requirements of the particle injection system are as follows: (1) compact size for installing on the holder of midplane manipulator whose diameter is approximately 86 mm, (2) compatibility with a strong magnetic field (<3 T) and a high vacuum environment ( $\sim 10^{-7}$  Torr), (3) capability to inject several mg of solid particles, and (4) a narrow particle injection angle.

The paper describes the device design and the device performance test in Sec. II. The diagnostics and analysis tool for the impurity transport study in KSTAR are given in Sec. III and a summary is presented in Sec. IV.

### II. DEVICE DESIGN AND PERFORMANCE

#### A. Device design

Figure 1 shows a schematic view of the particle injection system for KSTAR. The system consists of a particle injection gun, a trigger, a piezoelectric motor, and a particle storage compartment. A compressed spring is installed inside the particle injection gun and generates elastic force to push particles out. Two holes are prepared in the piston: one is a cylindrical hole of 4 mm in diameter and 5 mm in length inside the piston to store particles and the other is on the upper side of the piston for reloading particles from the particle storage. Due to the high tolerance for strong magnetic fields having low magnetic permeability, a piezoelectric motor (PUMR40, Piezo Technology©) and SUS316 material were chosen for components of the particle injection system. The metallic bar revolves on the shaft of piezoelectric motor to move the trigger. The bar presses backward and releases the trigger, and then elastic force generated by the compressed spring

<sup>a)</sup>Contributed paper, published as part of the Proceedings of the 20th Topical Conference on High-Temperature Plasma Diagnostics, Atlanta, Georgia, USA, June 2014.

<sup>b)</sup>Author to whom correspondence should be addressed. Electronic mail: wchoe@kaist.ac.kr.

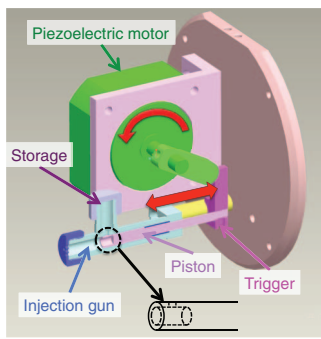


FIG. 1. Schematic view of the particle injection system.

ejects particles to the plasma. The diameter and length of the injection gun are 8 mm and 50 mm, respectively. The dimensions of particle injection system are designed to be about  $60 \text{ mm} \times 30 \text{ mm}$  for installation on a manipulator whose diameter is approximately 86 mm.

### B. Performance test in vacuum environment and magnetic field

The operation of the particle injection system in high vacuum environment was tested in a small vacuum chamber of  $6 \times 10^{-6}$  Torr. Note that typical KSTAR discharges have a vacuum of  $\sim 10^{-7}$  Torr. The driving test of the piezoelectric motor under a strong magnetic field was successfully carried out in a nuclear magnetic resonance device with a magnetic field strength of about 7 T. The field direction was perpendicular to the piezoelectric motor as it would be in KSTAR. Therefore, it was expected that the particle injection system work as designed in a high vacuum and strong magnetic field.

### C. Injection performance test

A test for flight-distance and distribution of launched particles was performed at atmosphere pressure (1 atm). Figure 2 shows a schematic view of the experimental setup for the injection performance test. The central axis indicates an extended line from the center of the particle injection gun. The target plate is 10 cm away from the gun position ( $l = 10 \text{ cm}$  in Fig. 2). A piece of adhesion tape is adopted on the target plate to catch particles. Copper (Cu,  $Z = 29$ ) and W ( $Z = 74$ ) particles are used for the demonstrated injection of low- and high- $Z$  impurity particles, respectively.

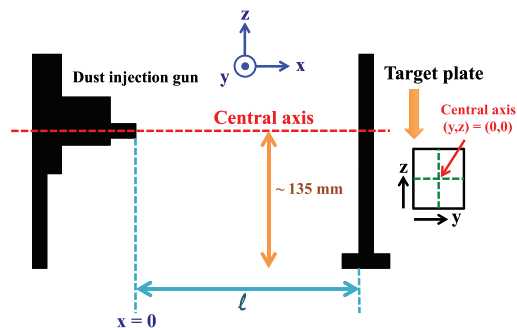


FIG. 2. Schematic view of the experimental setup.

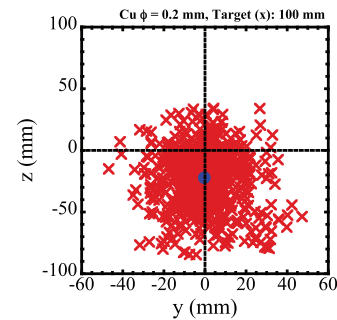


FIG. 3. Example of distribution of ejected Cu particles on the target plate and the average drop.

The cylinder-shaped Cu particles whose diameter and length are approximately 0.2 mm and 1 mm are used. The number of injected Cu particles is about 3 per mg. We varied the loading amount of Cu as follows: 5 mg, 10 mg, 15 mg, and 20 mg. For each case, Cu particles were ejected six times. The percentage of Cu particles reaching the target plate was over 70%; 93%, 88%, 83%, and 70% for the cases of 5 mg, 10 mg, 15 mg, and 20 mg, respectively. For the case of W, three different kinds of cylinder-shaped W particles, whose diameters are 0.06 mm, 0.1 mm, and 0.2 mm, were tested. The numbers of injected W particles for 0.06 mm, 0.1 mm, and 0.2 mm of diameter are approximately 2, 5, and 12 per mg, respectively. Tungsten particles were ejected five times. The amount of W particles that reached the target plate was over 95% and this did not depend on the amount or size of the W particles. For KSTAR experiments, impurity particles will be injected in doses of several mg, therefore it is expected that over 90% of particles will reach LCFS for typical discharges. Figure 3 shows a typical distribution of Cu particles on the target plate with the loading of 20 mg as an example. The central axis is plotted on the target plate as  $(y,z) = (0,0)$  in Fig. 3. The average drop is evaluated as an average distance from the central axis of all deposited particle positions (see the blue circle in Fig. 3). The launched particles were deposited at a slightly lower position than the central axis on the target plate. Most Cu particles are deposited in a range of  $-40 \text{ mm} < y < -40 \text{ mm}$  and  $-60 \text{ mm} < z < 20 \text{ mm}$ . Figure 4 shows the average drop as a function of the amount of Cu and W particles. The errors of the average drop were estimated from the standard deviation of the particle positions. The average drops of the Cu particles whose  $\phi = 0.2 \text{ mm}$  are in the range from  $-5 \text{ mm}$  to  $-25 \text{ mm}$  and increase with the increase in the particle amount. In the case of W particles, there is no sufficient difference found in the experiment and shows a constant average drop of about  $-10 \text{ mm}$ . Tungsten particles were distributed in the range of  $-15 \text{ mm} < z < 0 \text{ mm}$ . Here, a negative value means the lower direction from the central axis ( $-z$  direction). Note that there are two free parameters: size and density of particles to increase total mass load. Figure 5 shows the average drops as a function of the diameters of W particles. The average drop of W particles is about  $-10 \text{ mm}$  and it almost did not change with its size.

The error bar of the Cu particle case was larger than the W case as shown in Fig. 4 for  $\phi = 0.2 \text{ mm}$ . The distribution of

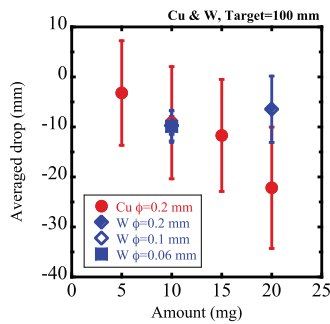


FIG. 4. Average drops as a function of the amount of Cu and W particles.

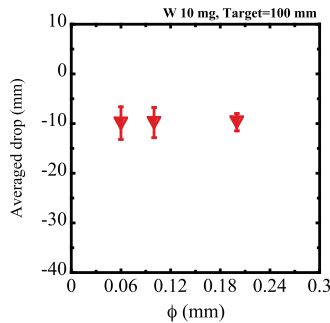


FIG. 5. Average drops as a function of diameter  $\phi$  of W particles.

W particles is narrower than that of Cu particles. Although the average drop increases with the amount of Cu particles, this dependence is not found with W particles. The mass densities of Cu and W are  $8.94 \text{ g/cm}^3$  and  $19.25 \text{ g/cm}^3$ , respectively, meaning that the number of Cu particles is at least twice larger than that of W particles. Average elastic energy delivered by the injection gun is 2 times less for Cu particles of the same mass (i.e., 10 mg) than that of W particles. It seems that the injection gun could deliver enough energy up to 10 mg of Cu particles (almost equivalent number of 20 mg of W particles) for 10 cm of flight distance. Because there are four times more particles in 20 mg Cu than in 10 mg W, the average energy delivered to each particle is 1/4. Therefore, they cannot fly away, but fall down quickly resulting in a large drop. In this device performance test, the average drops of Cu and W particles were approximately from  $-5$  to  $-25$  mm. The maximum allowable average drop was approximately 90 mm for this particle injection system, where impurity particles clash with the passive stabilizer of KSTAR. Therefore, the measured average drop is an acceptable level for KSTAR. The average initial velocities of Cu and W particles, which are evaluated from the average drop, were roughly 2–4 m/s ignoring air resistance.

### III. DIAGNOSTICS AND ANALYSIS TOOL FOR IMPURITY TRANSPORT STUDY IN KSTAR

To measure the impurity emission spectra, SXR and VUV diagnostics have been developed and installed in KSTAR. The ITER proto-type VUV diagnostic system that measures the emission spectra at the wavelengths of 14.4–60.0 nm, were installed in KSTAR. This survey diagnostics has a single channel whose line of sight passes through

near the plasma center, and the time resolution is 13–40 ms. The SXR array system has 2 arrays 32 channels, and 4 new arrays<sup>11</sup> of 256 channels have been prepared for the high-Z impurity transport study in 2014 KSTAR campaign. The spatial and time resolutions of the SXR system are approximately 2 cm and  $2 \mu\text{s}$ , respectively. Experimental transport coefficients, such as impurity diffusion coefficients and convection velocities, were evaluated by comparing the measured impurity emission spectra by the SXR array and the VUV diagnostics with the simulated ones by Stand Alone Non-CORONA (SANCO) code.<sup>10</sup>

Solid doses of different impurities, such as W, Cu, and C, will be injected by the particle injection system in KSTAR. The  $Z_{\text{eff}}$  dependence on the impurity transport will be studied as a next step. Analysis on the evaporation and trajectories of injected particles will be also addressed in future works.

### IV. SUMMARY

We have developed a gun-type particle injection system that will be installed on the manipulator at the D-port of KSTAR. This system satisfies the following requirements: (1) a compact size for installation on the holder of midplane manipulator, (2) compatibility with a strong magnetic field ( $<7$  T) and a high vacuum environment (by  $6 \times 10^{-6}$  Torr), (3) capability to inject approximately several mg of solid powders with a narrow particle injection angle, and (4) the target flight-distance, which is more than 10 cm, achieved with small particle loss of less than 10%. This particle injection system will be used for the impurity transport study in KSTAR.

### ACKNOWLEDGMENTS

One of authors (H. Y. Lee) is grateful to Dr. Juhung Kim at Korea Advanced Institute of Science and Technology, Dr. S. Morita and Dr. T. Ohishi at National Institute for Fusion Science, Japan for fruitful discussions and comments. This research was partially supported by National R&D Program through the National Research Foundation of Korea (NRF) funded by the Ministry of Science, ICT, of Republic of Korea (No. 2009-0082624). This study was also partially supported by Korea Research Council of Fundamental Science and Technology (KRCF) under the R&D program for international collaboration in Asian countries (No. PG1314).

<sup>1</sup>E. J. Dolye *et al.*, *Nucl. Fusion* **47**, S18 (2007).

<sup>2</sup>L. D. Horton *et al.*, *Nucl. Fusion* **39**, 993 (1999).

<sup>3</sup>A. S. Kukushin *et al.*, *Nucl. Fusion* **42**, 187 (2002).

<sup>4</sup>J. Hong *et al.*, “Control of core argon impurity profile by ECH in KSTAR,” *Nucl. Fusion* (unpublished).

<sup>5</sup>J. Kwak *et al.*, *Nucl. Fusion* **53**, 104005 (2013).

<sup>6</sup>S. H. Lee *et al.*, *Rev. Sci. Instrum.* **83**, 10E512 (2012).

<sup>7</sup>C. R. Seon *et al.*, *Rev. Sci. Instrum.* **81**, 10E508 (2010).

<sup>8</sup>H. Yamada *et al.*, *Fusion Eng. Des.* **49**, 915 (2000).

<sup>9</sup>D. K. Mansfield *et al.*, *Fusion Eng. Des.* **85**, 890 (2010).

<sup>10</sup>L. Lauro-Taroni *et al.*, *21st EPS Conference on Controlled Fusion and Plasma Physics* (Montpellier, 1994), p 102.

<sup>11</sup>S. H. Lee *et al.*, “Installation of soft X-ray array diagnostics and its application to tomography reconstruction using synthetic KSTAR X-ray images,” *Rev. Sci. Instrum.* (these proceedings).